PAPER

Check for updates

Artemisia herba-alba sesquiterpenes: *in silico* inhibition in the ATP-binding pocket†

Tarik A. Mohamed, [ID] *[a] Mohamed H. Abd El-Razek, [ID] [b] Ibrahim A. Saleh, [ID] [a] Sherin K. Ali, [ID] [a] Abeer A. Abd El Aty, [ID] [c] Paul W. Paré [ID] [d] and Mohamed-Elamir F. Hegazy [ID] *[a]

To identify antimicrobial leads for medical applications, metabolites from the aerial part of *Artemisia herba-alba* were extracted and chromatographically purified. Two new sesquiterpenes, 1β,8α-dihydroxyeudesm-4-en-6β,7α,11βH-12,6-olide (**1**) and 1β,6α,8α-trihydroxy, 11α-methyl-eudesma-4(15)-en-13-propanoate (**2**) along with a known eudesmanolide 11-*epi*-artapshin (**3**) were identified. Structures were determined by spectroscopic methods including 1D- and 2D-NMR as well as mass spectroscopy. Compound **3** inhibited Gram-positive bacteria *Bacillus subtilis*, *Lactobacillus cereus* and *Staphylococcus aureus* and exhibited antifungal activity against the pathogenic fungus *F. solani*. The mode-of-action of these antimicrobial sesquiterpenes as bacterial type II DNA topoisomerase and/or DNA gyrase B inhibitors were examined *via in silico* studies. Such molecular-docking studies were also employed to examine antifungal activity against an *N*-myristoyl transferase (NMT) target. Compound **3** had the greatest gyrase B binding affinity in the ATP-binding pocket and was found to possess an inhibitory action against non-invasive micro-test technology (NMT).

1. Introduction

Plant, microbial and marine natural products provide vital leads for drug discovery with more than 50% of currently authorized Western medications being derived from natural sources.[1] Medicinal herbs also have a rich tradition in ancient and Eastern pharmacopeias.[2] The family Asteraceae contains numerous plants rich in antioxidants and antimicrobials.[3–7] The genus *Artemisia* (Asteraceae) is a widely-dispersed genera, with over 500 varieties spread over temperate areas including North America, Europe, and Asia.[8] A number of recent phytochemical and pharmacological investigations utilizing species from *Artemisia*,[9–12] can be contributed, as least in part to the recognition of the sesquiterpenoid lactone artemisinin as a highly active natural product that serves as an effective treatment for malaria. The elucidation of this natural product as an anti-malaria treatment resulted in Tu Youyou being awarded the Nobel Prize in 2015.[13,14] Before the discovery of antibiotics, *Artemisia* was a common element in herbal tea blends, advised to TB patients to prevent sudation and later identified as the active component for chronic bronchitis.[15] Along with treating mental and neurological illnesses, the plant is used as an insecticide in the treatment of sweating, fever, rheumatism, and rheumatoid arthritis.[16,17] *Artemisia* is rich in terpenoids, flavonoids, coumarins, acetylenes, caffeoylquinic acids, and sterols. The plant has also been identified as having beneficial activity as an antimalarial, antiviral, antitumor, antipyretic, antihemorrhagic, anticoagulant, antianginal, antioxidant, antihepatitis agent.[18–23]

Computer-Aided Drug Designing (CADD) has gained great acceptance among biologists and chemists as a part of an interdisciplinary drug discovery approach. It plays an essential role in drug discovery, design, and analysis in the pharmaceutical industry. It is significantly used to reduce cost and speed up early-stage development of biologically new active molecules.[24] Recently, infections of resistant bacteria have become very common[25–27] and many pathogens; have become resistant to different classes of antibiotics.[27–29] A growing risk of antimicrobial resistance has provided a robust impetuous for identifying new antimicrobial agents with structural features different from existing antibiotics.[27,30] DNA gyrases have become an attractive target for anticancer and antibacterial research as they are essential enzymes for cell survival in prokaryotes. Searching for new inhibitors of the ATP-binding pocket of

[a]Chemistry of Medicinal Plants Department, National Research Centre, 33 El-Bohouth St., Dokki, Giza, 12622, Egypt. E-mail: tarik.nrc83@yahoo.com; elamir77@live.com; Tel: +20-11-275-39-989; +20-33-371-635

[b]Department of Natural Compounds Chemistry, National Research Centre, 33 El-Bohouth St., Dokki, Giza, 12622, Egypt

[c]Chemistry of Natural and Microbial Products Department, National Research Centre, 33 El-Bohouth St., Dokki, Giza, 12622, Egypt

[d]Department of Chemistry & Biochemistry, Texas Tech University, Lubbock, TX 79409, USA

Paper

gyrase B enzyme (PDB code 4GEE) is attracting the attention of the pharmaceutical industry.[31,32]

A. herba-alba, commonly known as white wormwood is a perennial dwarf shrub with greenish-silver leaves; it grows in dry and/or semi-arid areas.[33] In is found in North Africa, Spain, the Sinai Peninsula, Middle East, Northwestern Himalayas, and India; it is also found along the Mediterranean Sea.[34] Since ancient times, the plant has been utilized in folk medicine; Moroccan traditional medicine uses it to treat arterial hypertension and/or diabetes.[34] The leaves can be prepared as an herbal tea as an analgesic, an antibiotic, an antispasmodic, and a hemostatic.[35] An ethanol extract is used for neurological problems with demonstrated GABAA-benzodiazepine receptor action.[36] Aqueous extracts have anti-initiation and anti-promotional action against tumors,[37] and a methylene chloride : methanol extract (1 : 1) exhibits antinociceptive activity.[38]

The plant is highly polymorphic with many documented chemotypes.[39] This is significant as differing compound profiles will occur for specific chemotypes with differing medical effects depending on the chemotype. Based on the distinct sesquiterpene lactone profile observed in plant samples collected, we propose the emergence of a new *A. herba-alba* chemotype that is present in the south of the Sinai (Saint Catherine district), Egypt.

2. Results and discussion

2.1. Identification and structure elucidation

Chromatographic fractionation and purification of an organic extract of *A. herba-alba* afforded two new sesquiterpenes, 1β,8α-dihydroxyeudesm-4-en-6β,7α,11βH-12,6-olide (**1**) and 1β,6α,8α-trihydroxy, 11α-methyl-eudesma-4(15)-en-13-propanoate (**2**) along with a known eudesmanolide 11-*epi*-artapshin (**3**) (Fig. 1).[40]

Compound **1** was purified as a clear gum with $[\alpha]_D^{25} = +46.5$ (MeOH; $c = 0.5$); the chemical formula $C_{15}H_{22}O_4$ was identified from the HRESIMS ion peak at m/z 267.1518 (calcd 267.1522). Twenty-two protons and fifteen carbon resonances were identified based on ^{1}H and ^{13}C NMR data (Table 1). The ^{13}C NMR and DEPT spectra revealed three quartets, three triplets, five doublets, and four singlets. According to the IR spectrum, there is hydroxyl functionality at ν_{max} 3300 and 3560 cm^{-1}, as well as a γ-lactone carbonyl ring at ν_{max} 1770 and 1785 cm^{-1}. An HSQC experiment confirmed three methyls classified as: [one tertiary (δ_H/δ_C 1.03 s/19.6); one secondary (δ_H/δ_C 1.27 (d, $J = 7.7$ Hz)/9.4); and one vinylic (δ_H/δ_C 1.78 s/19.6)]; three saturated methylenes

were [δ_H/δ_C 1.63 m, 1.66 dd ($J = 14.0, 5.0$ Hz)/26.4, δ_H/δ_C 2.15 td (11.7, 7.7), 1.95 brdd ($J = 14.0, 3.5$ Hz)/33.4 and δ_H/δ_C 1.13 t ($J = 12.9$ Hz), 2.26 dd ($J = 12.9, 4.5$ Hz)/47.8] and five methines three of them were oxygenated methines [δ_H/δ_C 3.44 dd ($J = 12.4, 4.4$ Hz)/77.1, δ_H/δ_C 4.73 brd ($J = 11.7$ Hz)/80.0 and δ_H/δ_C 3.89 td ($J = 11.7, 4.1$ Hz)/64.7] and the other two were aliphatic methines [δ_H/δ_C 2.10 dddd (14.0, 11.5, 3.5, 1.5)/54.6 and δ_H/δ_C 2.78 dq ($J = 7.7, 7.7$ Hz)/36.8]. The resonance frequencies for four non-protonated carbons were also observed in the ^{13}C NMR spectra (Table 1); two of them olefinic at δ_C 126.9, a third was an aliphatic carbon at δ_C 41.0 and a fourth was a carbonyl unit at δ_C 180.0. In accordance with the above ^{1}H and ^{13}C NMR data (Table 1), compound **1** contains an eudesmane skeleton, with five degrees of unsaturation assigned to a double bond and a carbonyl while the other degrees of unsaturation are due to the tricyclic frame skeleton. Two spin systems, H-1-H-2-H-3 and H-6-H-7(H-11-H-13)-H-8-H-9, were identified in the ^{1}H–^{1}H COSY spectrum (Fig. 2). H$_2$-2 (δ_H 1.66, 1.63) was correlated with a single oxygenated methine proton (δ_H 3.44, H-1) and vicinal protons (δ_H 2.15, 1.95, H$_2$-3) leading to the initial spin system of C1(H)O–C2(H2)–C3(H2). In the second spin system, H-7 (δ_H 2.10) is coupled with H-6 (δ_H 4.73) and H-8 (δ_H 3.89), which in turn is coupled to H$_2$-9 (δ_H 1.13, 2.26) (Fig. 2). This establishes connectivity between C-1 and C-3 as well as C-6 and C-9. The alpha methine proton of the γ-lactone ring (δ_H 2.10, H-7) correlates with a secondary methyl (δ_H 1.27, Me-13) and an aliphatic oxygenated methines located at the β-position adjacent to it in the ^{1}H–^{1}H COSY spectrum. The HMBC correlations (Fig. 2) of H-3/C-15, C-4; H-6/C-4, C-5; and H$_2$-9/C-10, C-1, C-14 indicated a linkage between C-3 and C-5 *via* C-4 and between C-1 and C-9 *via* C-10 with a double bond between C-4 and C-5. The oxymethine group at δ_H 3.44 was assigned to C-1 based on HMBC long-range couplings between H$_3$-14 (δ_H 1.03) and C-1 (δ_C 77.1), as well as between H-1 (δ_H 3.44) and C-3 (δ_C 33.4) and C-5 (δ_C 126.9). According a doublet coupling pattern ($J = 11.7$ Hz) and an HMBC cross-peak between H-7 (δ_H 2.10) and C-6, the second oxymethine group at δ_H 4.73 was assigned to C-6 (δ_C 80.0). Since C-8 is unique with a vicinal proton–proton couplings with three protons, the coupling pattern at δ_H 3.89 td ($J = 11.7, 4.1$ Hz) established an oxymethine unit. HMBC correlations between H-8 (δ_H 3.89) and C-7, C-9, C-10, C-6 and C-11, corroborated with a hydroxyl group at C-8. A HMBC coupling between C-5 and C-10 was identified *via* correlation of CH$_3$-14 with C-5, H$_2$-9 with C-5, and H-6 with C-10. The COSY couplings of CH$_3$-13 and H-11, together with the agreement of H-11 HMBC correlations with C-12, C-7 and C-6, as well as de-shielding of C-12 at δ_C 179.94, indicated a γ-lactone ring. The NOESY data (Fig. 3) and coupling constants established the relative stereochemistry. Based on biogenetic precedent and in accordance with previously documented NMR chemical shifts for related sesquiterpene lactones, H-7 relative stereochemistry was assigned to an α-configuration.[22] The large vicinal coupling ($J = 11.7$ Hz) indicated a *trans* H-6-H-7 conformation. The multiplicity on the chemical shift of the doublet characteristic for H-6 suggested a *trans*-eudesmane-12,6-olide. Based on COSY, HMBC, coupling constant and comparison with the previously eudesmanolides reported,[22] the double doublets at δ_H 3.44 ($J =$
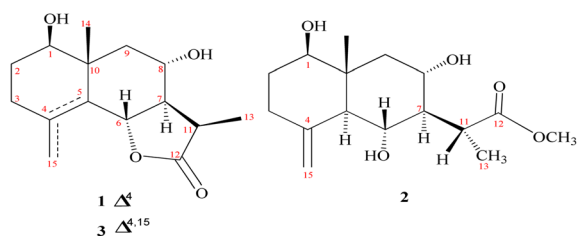

Fig. 1 Identified metabolites (**1–3**).

Table 1 ^{1}H NMR and ^{13}C NMR spectroscopic data for **1–2** with CDCl$_3$ as the solvent

| No.	**1** δ_C	δ_H (J in Hz)	**2** δ_C	δ_H (J in Hz)
1	77.1	3.44 dd (12.4, 4.4)	78.3	3.38 dd (4.1, 10.7)
2$_{axi}$	26.4	1.63 m	31.5	1.49 dddd (14.0, 11.0, 10.7, 4.3)
2$_{eq}$		1.66 dd (14.0, 5.0)		1.74 m
3$_{axi}$	33.4	2.15 td (11.7, 7.7)	34.9	2.02 m
3$_{eq}$		1.95 brdd (14.0, 3.5)		2.35 m
4	126.9	—	145.1	
5	126.9	—	54.7	1.80 brd (10.6)
6	80.0	4.73 brd (11.7)	65.4	3.78 t (10.6)
7	54.6	2.10 dddd (14.0, 11.5, 3.5, 1.5)	54.4	2.00 t (11.0)
8	64.7	3.89 td (11.7, 4.1)	65.6	3.55 td (11.7, 4.1)
9$_{axi}$	47.8	1.13 t (12.9)	45.7	1.15 t (11.7)
9$_{eq}$		2.26 dd (12.9, 4.5)		2.33 dd (11.7, 4.3)
10	41.0	—	40.8	
11	36.8	2.78 dq (7.7, 7.7)	36.1	3.17 q (6.9)
12	180.0	—	178.6	
13	9.4	1.27 d (7.7)	10.5	1.12 d (6.9)
14	19.6	1.03 s	12.7	0.67 s
15	19.6	1.78 s	108.4	4.67 brd (1.5)
				4.97 brd (1.5)
OCH$_3$			52.0	3.64 s
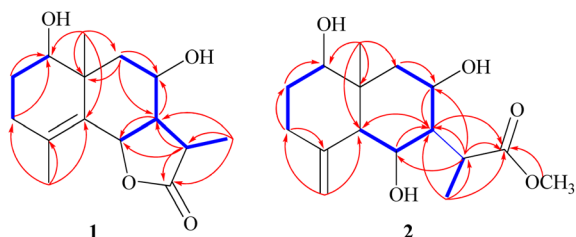
Fig. 2 Observed ^{1}H–^{1}H COSY and HMBC correlations (shown in blue and red, respectively) for **1–2**.
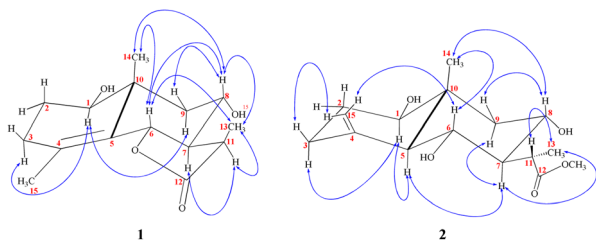
Fig. 3 Observed NOESY correlations for **1–2**.

12.4, 4.4 Hz) originates from an axial proton at C-l, geminal to an OH group and a triplet doublet at δ_H 3.89 (J = 11.7, 4.1 Hz) indicating that the carbinol proton (H-8) is in an anti-periplanar orientation. These spectroscopic results supported an eudesmane-type sesquiterpene lactone. The NMR findings (Table 1) are comparable to those for 1β,8α-dihydroxyeudesm-4-en-6β,7α,11βH-12,6-olide.[41] Actually, the former compound was diagnosis from a mixture with other compounds and could be

obtained from 8α-hydroxytaurin by reduction with sodium borohydride. The distinguishing signal for C-11 was discovered by a comparison between the biodiversity of such species and data from the literature.[42]

The stereochemistry at C-11 was established using the value of the NMR coupling between H-7 and H-11.[42] The C-11 proton of 1β,8α-dihydroxyeudesm-4-en-6β,7α,11βH-12,6-olide,[41] appears as a double quartet at δ_H 2.34. The J_{H7-11} = 11.7 Hz and J_{H11-13} = 7.0 Hz frequencies represent the X of the A$_3$MX pattern. In accordance with the Newman projection, the C-11 proton is positioned in a pseudo-axial orientation (Fig. 4A). As seen in Fig. 4B, the C-11 proton moves into a pseudo-equatorial orientation and the pattern changes to be located at δ_H 2.78 with J_{H7-11} = 7.7 Hz. Based on spectral data for **1** in comparison with 1β,8α-dihydroxyeudesm-4-en-6β,7α,11βH-12,6-olide,[41] the two
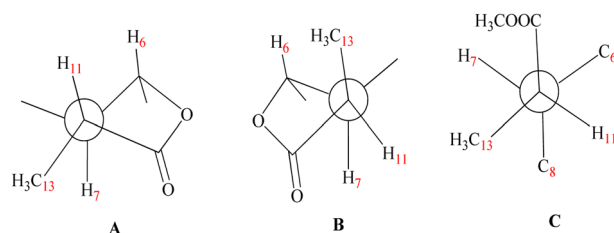
Fig. 4 Newman projections [A] H-11 displays data for the coupling constants (J_{H7-11} = 11.7 Hz) and (J_{H11-13} = 7.0 Hz) in a pseudo-axial orientation. [B] (J_{H7-11} = 7.7 Hz) and (J_{H11-13} = 7.0 Hz) are values of the coupling constants which might be seen in the pseudo-equatorial configuration of H-11. [C] Confirmed that compound **2** virtually completely dismisses the coupling between H-7 and H-11.

compounds are epimeric eudesmanolides. However, significant downfield changes in the signals of H-6, H-7, and H-11, along with a significant upfield shift of the Me-13 are seen for **1**, together with a decline in the coupling constant from 11.7 Hz in 1β,8α-dihydroxyeudesm-4-en-6β,7α,11βH-12,6-olide,[41] to 7.7 Hz in **1**. The inverted order of the Me-13 absorption observed in the NMR spectra, where the resonance of Me-13 equatorial (sharing a co-planarity with C-12, Fig. 4A) is found further downfield (Δ_{δ_H} = +0.12 ppm) than that of **1**, is attribute to the anisotropic deshielding effect of the carbonyl group that is a component of the γ-lactone ring (Fig. 4B). ^{13}C NMR spectral comparisons between **1** and 1β,8α-dihydroxyeudesm-4-en-6β,7α,11βH-12,6-olide[41] shows significant differences in some chemical shifts (Table 1). These changes include an up-field shift for C-7 (Δ_{δ_C} = −4.0 ppm), C-8 (Δ_{δ_C} = −6.3 ppm) and C-11 (Δ_{δ_C} = −4.0 ppm), as well as C-13 (Δ_{δ_C} = −5.0 ppm). The methyl equatorial nature (Fig. 4A) results in a decrease in the β-effect on C-7 and γ-effect on C-8, as predicted, causing downfield shifts C-7 and C-8 in comparison with **1**. NOESY data (Fig. 3) validated the relative stereochemistry for **1** with the opposite configuration for the C-12 stereogenic center, as well as changes in the coupling constant for H-12. Thus, **1** is indeed a 12-epimer of 1β,8α-dihydroxyeudesm-4-en-6β,7α,11βH-12,6-olide.

Compound **2** is a colorless oil with a positive optical rotation $[\alpha]_D^{25}$ = +55.2 (MeOH; c = 0.5). A prominent IR band at 1740 cm^{-1} indicated a carbonyl ester group, while broad band's at ν_{max} 3300 and 3560 cm^{-1} suggested free hydroxyl functionality. Other bands at ν_{max} 3090, 1650, and 900 cm^{-1} were attributed to the di-substituted carbon–carbon double bond (C=CH$_2$). HRESIMS (m/z 299.1782) analysis indicated a molecular formula of C$_{16}$H$_{26}$O$_5$ and ^{13}C NMR data (Table 1) was consistent with an additional carbon deviating from the common sesquiterpene carbon number and four degrees of unsaturation. One methyl ester was detected based on the ^{13}C and DEPT NMR [δ_C 178.6 (s), 52.0 (q)]. Additional signals at δ_C 145.1 (s), 108.4 (t), were attributed to an exocyclic double bond accounting for two degrees of unsaturation with a bicyclic frame accounting for the other degrees of unsaturation. ^{13}C NMR and DEPT data (Table 1), indicated two methyls (one of which was angular δ_C 12.7); and the other was secondary (δ_C 10.5), three sp^3 methylenes (δ_C 31.5, 34.9, and 45.7), six sp^3 methines, including three oxygenated carbons (δ_C 78.3, 65.4 and 65.6), as well as the other three aliphatics (δ_C 54.7, 54.3 and 36.1) and one sp^3 quaternary carbon at δ_C 40.8. These NMR findings complemented those of **1**, assuming that **2** contain an eudesmane skeleton. NMR signal similarity from C-1–C-10 suggests shared rings of eudesmane derivatives with the respect of the different position of a double bond. The exocyclic double bond $\Delta^{4,15}$ in **2** was replaced by a methyl group (Me-15) and relocated to be $\Delta^{4,5}$ as an olefinic bond in **1**. This was demonstrated by the lack of sp^2 methylene [δ_C 145.1(C-4); δ_H/δ_C 4.67 br d (J = 1.5 Hz, H-15a), 4.97 br d (J = 1.5 Hz, H-15b)/δ_C 108.4 (C-15)] in **1** and the presence of one vinylic methyl (CH$_3$-15) [δ_H/δ_C 1.78 s/19.6] and two sp^2 quaternary carbons (δ_C 126.9). Also, in **2**, the γ-lactone ring was missing with instead an ester side chain. HMBC and ^{1}H–^{1}H COSY data (Fig. 2) indicated connectivities between these units. Three isolated proton spin systems that correspond to the

C-1/C-2/C-3, C-5/C-6/C-7/C-8/C-9, and C-11/C-13 subunits of structure **2** were observed. An eudesmane moiety containing a $\Delta^{4,15}$ double bond was created by the HMBC correlations of H-1 with C-10 and C-9, H-14 with C-1, C-5 and C-9, H-3 with C-5, H-15 with C-3 and C-5, and H-7 with C-11 and C-12. A 7-propanoate moiety was ascribed as a result of correlations between H-13, C-11, C-7, and the carbonyl ketone C-12, as well as between H-11, C-7, C-6, C-8, and the methoxy group. And furthermore, it was proposed based on HMBC correlations of H-7 with C-11, C-13, and carbonyl ester C-12 that the propanoate moiety and the eudesmane skeleton are linked at C-7. The HMBC connection between the methoxy group at δ_H 3.64 and C-13 (δ_C 178.6) established that it is a component of a methyl ester group. H-7 relative stereochemistry was ascribed to the α-configuration based on biogenetic precedence and in agreement with previously recorded NMR chemical shifts for associated sesquiterpene lactones.[22] The *trans*-5,6/*trans*-6,7 disposition in **2**, was consistent with the well-defined triplet at configuration δ_H 3.78 (J = 10.6 Hz) that was produced by the carbinol proton at C-6. The key distinctions between **1** and **2** was the emergence of a propanoate moiety coupled with C-7 in **2** and the elimination of the γ-lactone ring that is part of the skeleton in **1**. The up-field shifted of H-6, H-7, and H-8 combined with a down-field H-11 for **2** served as confirmation of this assignment. The aspect of the signal from H-11 that was supposed to have arisen as a quintuplet (J = 7.5, 7.5 Hz) at coupled with C-7 in **2** and the elimination coupled with C-7 in **2** and the elimination δ_H 2.21, or rather, as a double quartet at 1.67 (J = 12.0, 7.0 Hz), in many eudesman skeletons a downfield shift to δ_H 3.17 is observed with a reduction of the coupling constant equal to 6.9 Hz. Additionally, the multiplicity of the H-7 signal that appears as a triplet at δ_H 2.00 (J = 11.0 Hz) and a quartet signal at δ_H 3.17 (J = 6.9 Hz) characteristic for H-11, that confirmed the equatorial orientation of the propanoate moiety at C-7 with a dihedral angle between the two vicinal protons (H-7 & H-11) being close to 90° (Fig. 4C). As a result, it is possible to reveal the Me-13 as having an α-orientation. A stereoisomer of **2** has been previously isolated from *A. illicola*[43] with the trivial name of sericin methyl ester A. The stereochemistry of sericin methyl ester A was determined by X-ray with C-11 being pro-*S*. By ^{13}C NMR comparisons, C-11 of **2** was assigned to an *R*-configuration with a shift changes of +4.0 ppm along with a change in multiplicity from doublet quartet to be quartet. The NOSY correlation (Fig. 3) between CH$_3$-13 and H-7, also was consistent with a H-11 β-orientation. The NOESY spectrum showed distinct interactions between H-1 (δ_H 3.38)/H-5 (δ_H 1.80)/H-3$_{axi}$ (δ_H 2.02), which showed that H-1 is in an α-orientation. Significant evidence for the β-orientation of H-6 and H-8 were derived by correlations between H-6 (δ_H 3.78) and CH$_3$-14 (δ_H 0.67), and between H-8 (significant evidence δ_H 3.55) with CH$_3$-14 (δ_H 0.67) and H-9$_{eq}$ (δ_H 2.33). Based on the aforementioned data, **2** was identified as 1β,6α,8α-trihydroxy,11α-methyl-eudesma-4(15)-en-13-propanoate. The 11,12-hydrogenation pattern for an un-lactonized sesquiterpene is rare, particularly with hydroxylation at C-8.

2.2. Chemosystematic significance

The taxonomy of the genus *Artemisia* had already sparked debate. Several researchers have divided the genus into different taxa below the genus level.[44,45] For particular, *Artemisia* was split into three subgenera:[46] *Artemisia*, *Seriphidium* Besser, and *Dracunculus* Besser. *Tridentatae* (Rydb.) McArthur, a novel group that is solely found in North America, was introduced by McArthur *et al.*[47] Others like,[46] have traditionally classified the genus *Artemisia* into three subgenera: (1) *A.* subg., all of the blooms on *Artemisia* are fertile, the marginal ones are female, and the center ones are hermaphrodite. It has heterogamous capitula; (2) *A.* subg. *Dracunculus* has heterogamous capitula, a glabrous receptacle, marginal female flowers, centre hermaphrodite blooms, and all or some of the inner flowers are fertile; and (3) *A.* subg. *Seriphidium* has hermaphrodite blooms throughout and a homogamous capitula with a glabrous receptacle. Valles and McArthur (2001)[45] categorized *Artemisia* into the five groupings, mostly based on capitula type and floret fertility: *Tridentatae*, *Absinthium* DC., *Artemisia*, *Dracunculus*, *Seriphidium*, and (Rydb.) *Seriphidium* and *Artemisia* were separated to form a new genus by Ling[48–50], acknowledged this division; nevertheless, *Seriphidium* and *Artemisia* were once more joined by Watson *et al.* in 2002.[51] Internal transcribed spacers (ITS) of nuclear ribosomal DNA and chloroplast DNA (cpDNA) restriction site variation have both been used in molecular research to explore this separation.[52] However, there is still considerable debate over how to classify *Artemisia* and the interactions between its many components.[52]

The aerial parts of *A. herba-alba* stored many structural varieties of sesquiterpene lactones. The most common lactone types in this species are eudesmanolides and germacranolides, respectively. In all, there are 64 sesquiterpene lactones, of which 41 are eudesmanolides and around 23 are germacranolides.[22,34] Investigation of *A. herba-alba* plants in Israel's Negev and Judean desert led to the identification of five distinct chemotypes based on variations in their sesquiterpene lactone composition.[34] Segal and colleagues studied the chemotypes of *A. herba-alba* gathered in various places in Egypt and Israel and discovered many novel germacranolides and eudesmanolides, known as herbolides A–J.[53,54] There were confirmed to be 10 sesquiterpene lactones, of which 3 were eudesmanolide skeleton.[34] Sesquiterpene lactones (37) from *A. herba-alba*, (31 of which were eudesmanolide) collected in various geographic locations, have been the subject of certain phytochemical research in Spain.[34] The presence of oxygen functions at C-9 (germacrane and eudesmane numbering) in lactones from the African specimens, markedly different compounds from Spain and those obtained by Segal *et al.*[53,54] These sort of lactones were not uncovered from plant material gathered in the Sinai desert.[55] However, a study on an Egyptian specimen produced a few novel sesquiterpene lactones, with two of them having oxygen functionalities at C-9.[56] The findings reported from Spain suggest that lactones isolated from North African *A. herba-alba* may in fact have a unique chemical property called oxygenation at C-9. *A. herba-alba* growing in Egypt has been the subject of several studies on its chemistry. Sesquiterpene lactones have been the subject of the majority of investigations. All lactones identified (of which 4 eudesmanolides and 5 germacranolides) are different from those previously found in Israel-grown *A. herba-alba*. All collections, apart from one, were found to be 1,3-dihydroeudesmanolides and 1,3-dihydrogermacranolides containing at least an oxygen function at C-9, a rare characteristic in the genus *Artemisia*. However, the instance under research totally lacks the eudesmanolides oxygenated at C-9, which are among the most distinctive chemical characteristics of the sesquiterpene lactones isolated from North African *A. herba-alba*.[34] Additionally, a range of sesquiterpene lactones with at least a C-8 oxygen function have been found in Egyptian *A. herba-alba* specimens. *A. herba-alba* species from Morocco (of which 2 eudesmanolides out of 6) and Algeria (of which 2 eudesmanolides) were examined chemically in a small number of literature studies, demonstrating the abundance of sesquiterpenes from this genus.[34] Eudesmanolides makes up over 60% of *A. herba-alba*, whereas germacranolides makes up around 35%. *Seriphidium* is a section of the genus *Artemisia* that contains *A. herba-alba*. These chemical characteristics of *A. herba-alba* are generally in accordance with what is anticipated for members of the section *Seriphidium*.[57,58] The pronounced propensity for the manufacture of 11,13-dihydroeudesmanolides is a characteristic of plants in this section.[34,57–59] However, the large prevalence of lactones with a 11αH stereochemistry is far less typical. It's interesting to note that the majority of the lactones identified in the Spanish subspecies of *A. herba-alba* match this structural characteristic. However, over the past several years, a variety of sesquiterpene lactones have been identified in *A. herba-alba* specimens from Egypt and Spain reflected that the percentage of eudesmanolides with a 11βH stereochemistry about 66% in contrast to 34% with 11αH stereochemistry. This reflects that the majority of the isolated eudesmanolides belong to 11αH stereochemistry. The published ^{13}C-NMR spectrum data, suggests that structures need to be updated. The chemical shift values for the atom C-13 in several the lactones are in the 9–10 ppm range. This indicates that these compounds are truly 11α,13-dihydrolactones since they feature a β-Me group at C-11.[60] We looked into *A. herba-alba*, which was gathered in Spain and North Africa, since we were intrigued by these variations in the chemical makeup, which may indicate taxonomic changes at the subspecies or even species level. We thus feel that the chemical information that is currently accessible supports our earlier findings that were based on morphological criteria.[61]

2.3. Antimicrobial activity

Results in Tables 2 and 3 indicated that **3** is the most effective against all tested bacteria with IZDs of 7–8 mm and MIC values 25–100 mg. Compounds **1** and **2** showed moderate antibacterial activity with IZDs around 7 mm against two bacterial strains. In addition, antifungal activity was observed (IZD 8 mm) and an MIC value of 25 for **3** (Tables 2 and 3). Moderate antifungal effects also observed with **1–2** (IZD 7 mm). In contrast, each compound was inactive against the *E. coli* and the yeast strain *C. albicans*. Compound **3** showed strong binding affinity

Table 2 Antimicrobial activity for **1–3**[a]

| | Inhibition zone diameter (IZD) (mm) | | | | | |
| | Bacterium | | | | Yeast | Fungus |
Compound	*B. subtilis* ATCC6633	*L. cereus* ATCC14579	*S. aureus* ATCC29213	*E. coli* ATCC 25922	*C. albicans* ATCC 10321	*F. solani* NRC15
1	N.A.	7 ± 0.6	7 ± 0.7	N.A.	N.A.	7 ± 1.4
2	7 ± 0.6	7 ± 0.7	N.A.	N.A.	N.A.	7 ± 0.6
3	7 ± 0.8	8 ± 0.2	8 ± 0.4	N.A.	N.A.	8 ± 0.00
Thiophenicol	20 ± 0.7	23 ± 0.0	18 ± 1.4	15 ± 0.7	N.A.	N.A.
Treflucan	N.A.	N.A.	N.A.	N.A.	22 ± 0.4	12 ± 0.7

[a] Values of inhibition are the average of three different points around the discs $\pm$ SD. N.A. No activity.

(-7.08 kcal mol^{-1}) with 4GEE, while compounds **1–2** showed more moderate binding (-6.7 and -6.8 kcal mol^{-1}, respectively). Additionally, the inhibition constant (pK_i) for the tested metabolites were: 11.6 μM, 9.9 μM and 6.4 μM, **1–3**, respectively (Fig. 5).

A single *N*-myristoyltransferase present in fungi, protozoa, and insects is essential for survival.[62,63] The binding score of **3** with the enzyme was the highest (-6.99 kcal mol^{-1}) and moderate with **1–2** (-6.8 and -6.1 kcal mol^{-1} respectively). The inhibition constants (pK_i) were 10.1, 34.6, and 7.5 μM, for **1–3**, respectively. With growing occurrence of antimicrobial resistance[25–29] a need to identify new classes of antimicrobial agents is essential.[27,30] DNA gyrases have become an attractive target for antibacterial research as they are essential enzymes for cell survival in prokaryotes. Today, searching for new inhibitors of the ATP-binding pocket of gyrase B enzyme (PDB code 4GEE) is attracting the attention of pharmaceutical industries.[31,32] The *N*-myristoyltransferase appears to be present in eukaryotes. Fungi, protozoa, and insects possess a single *N*-myristoyltransferase, essential for their survival, while mammals possess various *N*-myristoyltransferases (Fig. 6).[62,63]
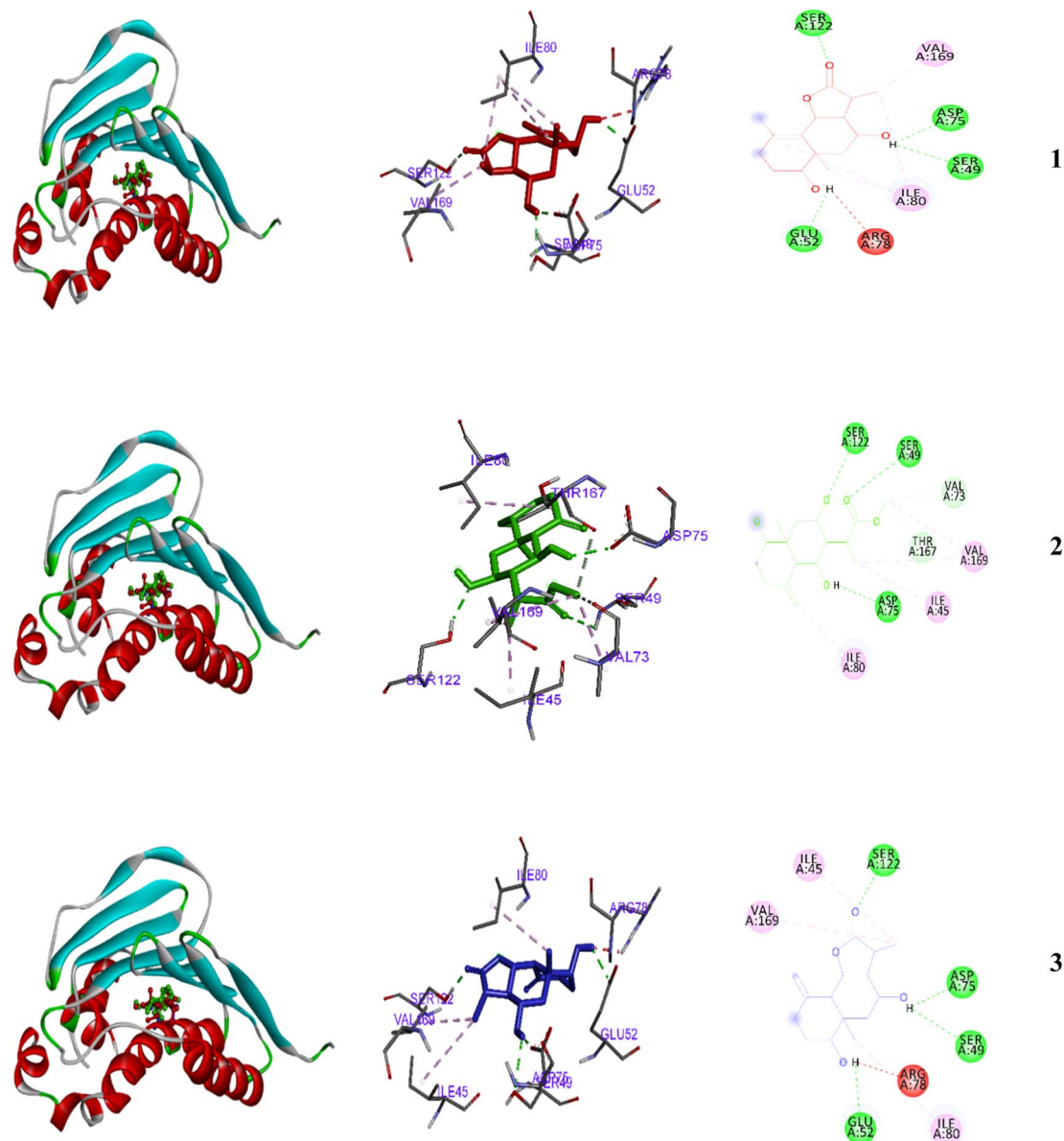
8100 spectrometer. For mass spectrometry measurements, IMS was performed on a Finnegan LCQ ion trap mass spectrometer and HR-EI-MS experiments were performed on Fourier transform ion cyclotron mass spectrometer. EI-MS experiments were performed a JEOL JMS-GCMATE mass spectrometer. Using tetramethylsilane as an internal standard, the ^{1}H (600 MHz) and ^{13}C (150 MHz) NMR spectra were achieved on a JEOL JNM-ECA 600 spectrometer. Compound separation for analytical and preparative separation was carried out using YMC-Pack ODS-A (250 × 4.6 mm i.d.) and (250 × 20 mm i.d.) columns, respectively. Purification was performed using a Shimadzu HPLC system furnished with a RID-10A refractive index detector. Fuji Silysia Chemical, Ltd.'s normal-phase silica BW-200 (Fuji Silysia Chemical, Ltd., 150–350 mesh) and Chromatorex's ODS reverse phase DM1020T (Fuji Silysia Chemical, Ltd., 100–200 mesh) were used for chromatography separations (Fuji Silysia Chemical, Ltd., 100–200 mesh). Additionally, silica gel 60 F$_{254}$ (Merck, 0.25 mm) and RP-18 WF$_{254}$ were used (Merck, 0.25 mm) for TLC analysis with compound visualization by with H$_2$SO$_4$–MeOH (1 : 9) spray followed by heating.

3. Experimental

3.1. General experimental procedures

For specific rotation, a Horiba SEPA-300 digital polarimeter (5 cm) was used and IR data was collected from a Shimadzu FTIR-

3.2. Plant material

A. herba-alba was harvested in June 2017 in the South Sinai (Saint Catherine) region of Egypt; a voucher specimen (SH-1109) was deposited in the herbarium of the protectorate of St. Katherine, Egypt.

Table 3 Minimal inhibitory concentration against pathogenic microbes for compounds **1–3**

| | Minimum inhibitory concentration (μg per disc) | | | |
| | Bacterium | | | Fungus |
Compound	*B. subtilis* ATCC6633	*L. cereus* ATCC14579	*S. aureus* ATCC29213	*F. solani* NRC15
1	—	100	50	100
2	50	50	—	50
3	100	25	50	25
Thiophenicol	3.13	3.13	3.13	—
Treflucan	—	—	—	50

Fig. 5 2D and 3D representations of the predicted binding modes inside the active site of the bacterial 4GEE for compounds **1–3**.

3.3. Extraction and isolation

Aerial stems and leaves (2.5 kg) were crushed and extracted for 2 days at room temperature with CH_2Cl_2–MeOH (1 : 1). The extract was concentrated *in vacuo* at 45 °C to produce a dark brown residue (200 g). The material was purified on a silica gel column (6 × 120 cm) with a gradient of *n*-hexane up to 100% $CHCl_3$ and $CHCl_3$–MeOH up to 50% MeOH (3 L of each solvent combination). To create two sub-fractions, the *n*-hexane : CH_2Cl_2 (1 : 1) fraction (8.3 g) was run over a second silica gel column (3 × 120 cm). Sub-fraction 1 A (2.3 g) underwent further HPLC purification and MeOH : H_2O elution (20 : 80). The flow rate was adjusted to 1.5 mL min^{-1} and was at 0–70 min to produce **1** (30 mg, purity > 97% by HPLC) (eluent CH_2Cl_2/ MeOH/H_2O 80 : 3 : 1, R_f = 0.30) and **3** (55 mg, purity > 97% by HPLC) (eluent CH_2Cl_2/MeOH/H_2O 80 : 3 : 1, R_f = 0.20), using an eluent ratio of 80 : 3 : 1. HPLC was used to further purify sub-fraction 2 A (1.2 g), which was eluted with MeOH : H_2O. (20 : 80). HPLC was further used to increase purity for **2** (40 mg, purity > 97% by HPLC) (eluent CH_2Cl_2/MeOH/H_2O 70 : 3 : 1, R_f = 0.20), the flow rate was adjusted to 2.0 mL min^{-1} and was at 0– 60 min.

3.4. Spectral data

3.4.1 1β,8α-Dihydroxyeudesm-4-en-6β,7α,11βH-12,6-olide (1). Clear gum, $[\alpha]_D^{25}$ = +46.5 (MeOH; *c* = 0.5); for ^1H (CDCl$_3$, 600 MHz) and ^{13}C (CDCl$_3$, 150 MHz) NMR, see Table 1; HRESIMS, *m/z* 267.1518, (calcd 267.1522, $C_{15}H_{22}O_4$); IR (ν_{max} cm^{-1}) = 3300, 3560 (OH), 1770 and 1785 (γ-lactone).

3.4.2 1β,6α,8α-Trihydroxy, 11α-methyl-eudesma-4(15)-en-13-propanoate (2). Colorless oil, $[\alpha]_D^{25}$ = +55.2 (MeOH; *c* =
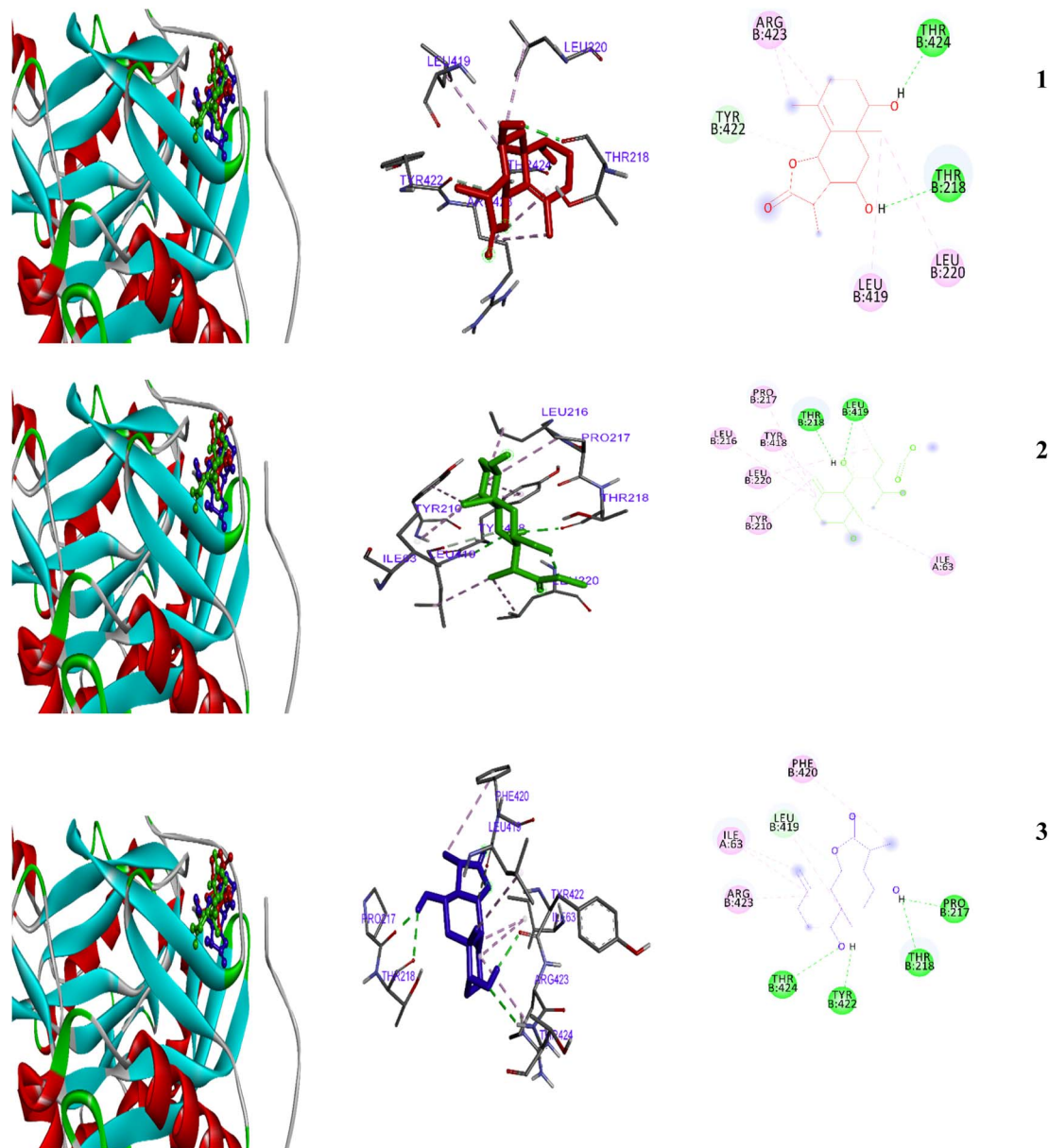
Fig. 6 2D and 3D representations of the predicted binding modes inside the fungal active site of 1IYK for compounds **1–3**.

0.5); for ^{1}H (CDCl$_3$, 600 MHz) and ^{13}C (CDCl$_3$, 150 MHz) NMR, see Table 1.; HRESIMS, m/z 299.1780, (calcd 299.1782, C$_{16}$H$_{26}$O$_5$); IR (ν_{max} cm^{-1}) = 3300, 3560 (OH), 1740 (C=O), 3090, 1650, 900 (C=C).

3.5. Antibacterial and antifungal assay

The antimicrobial activities were assayed *in vitro* against Gram positive (*Bacillus subtilis* ATCC6633, *Lactobacillus cereus* ATCC14579 and *Staphylococcus aureus* ATCC29213), Gram negative (*Escherichia coli* ATCC25922), yeast (*Candida albicans* ATCC10321), and fungi (*Fusarium solani* NRC15), using an agar diffusion technique.[22] Filter paper discs (5 mm in diameter) saturated with (100 µg/5 µL DMSO per disc) for the test compounds. Thiophenicol and treflucan are used as positive

controls for antibacterial and antifungal activity, respectively (100 µg per disc). The DMSO solvent negative control showed no inhibition zone. Prepared discs were placed on the surface of each plate, at a concentration of 1 × 10^6/mL of fungi (potato dextrose agar medium) and 1 × 10^8/mL of bacteria (nutrient agar medium). The plates left for 30 min at 4 °C and then incubated for 24 h at 30 °C for bacteria and 72 h at 28 °C for the fungus. The zone of inhibition zone was recorded at three different points and an average value are reported as mean ± SD.

3.5.1 Minimal inhibitory concentration (MIC). All compounds were evaluated for its minimal inhibitory concentration MIC at the final concentrations; 100, 50, 25 and 12.5 µg mL^{-1}. The lowest concentration showing inhibition zone

around the disc was taken as the minimum inhibitory concentration (MIC).

3.6. Molecular docking

The chemical structures of **1–3** were downloaded as SDF files from the PubChem database (https://pubchem.ncbi.nlm.nih.gov/(accessed on 29 January 2021)), and then converted to a PDB format *via* Avogadro software (https://avogadro.cc/). The protein crystal structures for 4GEE (antimicrobial) and 1Iyk (anti-fungal) were downloaded from the protein databank (https://www.rcsb.org/) using a previously published molecular docking protocol (Mohamed *et al.*, 2020).

4. Conclusions

Artemisia herba-alba afforded two new sesquiterpenes, 1β,8α-dihydroxyeudesm-4-en-6β,7α,11βH-12,6-olide (**1**) and 1β,6α,8α-trihydroxy, 11α-methyl-eudesma-4(15)-en-13-propanoate (**2**) along with a known eudesmanolide 11-*epi*-artapshin (**3**). Molecular docking simulations indicate that the natural-product antibiotic, eudesmanolide 11-*epi*-artapshin (**3**) can bind in the ATP-binding pocket to function as a gyrase B inhibitor; compound **3** also is able to bind as a fungal inhibitor to *N*-myristoyltransferase.

Author contributions

Conceptualization, T. A. M., M. H. A., P. W. P. and M.-E. F. H.; formal analysis, T. A. M., M. H. A., I. A. S., A. A. A. and M.-E. F. H.; investigation, T. A. M., M. H. A., S. K. A., A. A. A., P. W. P. and M.-E. F. H.; writing—original draft preparation, T. A. M., M. H. A., I. A. S., S. K. A., A. A. A. and M.-E. F. H.; writing—review and editing, T. A. M., M. H. A., I. A. S., S. K. A., A. A. A. and M.-E. F. H.; funding acquisition, T. A. M. All authors have read and agreed to the published version of the manuscript.

Conflicts of interest

The authors declare no conflict of interest.

Notes and references

1 D. J. Newman and G. M. Cragg, *J. Nat. Prod.*, 2016, **79**, 629–661.

2 S.-Y. Pan, G. Litscher, S.-H. Gao, S.-F. Zhou, Z.-L. Yu, H.-Q. Chen, S.-F. Zhang, M.-K. Tang, J.-N. Sun and K.-M. Ko, *Evid.-Based Complementary Altern. Med.*, 2014, **2014**, 1–20.

3 U. Anand, N. Jacobo-Herrera, A. Altemimi and N. Lakhssassi, *Metabolites*, 2019, **9**, 258.

4 U. Anand, S. Nandy, A. Mundhra, N. Das, D. K. Pandey and A. Dey, *Drug Resistance Updates*, 2020, **51**, 100695.

5 C. L. Gorlenko, H. Y. Kiselev, E. V. Budanova, A. A. Zamyatnin Jr and L. N. Ikryannikova, *Antibiotics*, 2020, **9**, 170.

6 Y. Zu, H. Yu, L. Liang, Y. Fu, T. Efferth, X. Liu and N. Wu, *Molecules*, 2010, **15**, 3200–3210.

7 D.-c. Hao and P.-g. Xiao, *Chin. Herb. Med.*, 2020, **12**, 104–117.

8 K. S. Bora and A. Sharma, *Pharmaceut. Biol.*, 2011, **49**, 101–109.

9 R. X. Tan, W. Zheng and H. Tang, *Planta Med.*, 1998, **64**, 295–302.

10 M. Willcox, *J. Altern. Complementary Med.*, 2009, **15**, 101–109.

11 B. Koul, P. Taak, A. Kumar, T. Khatri and I. Sanyal, *J. Glycomics Lipidomics*, 2017, **7**, 142.

12 H. Ekiert, J. Świątkowska, E. Knut, P. Klin, A. Rzepiela, M. Tomczyk and A. Szopa, *Front. Pharmacol.*, 2021, **12**, 653993.

13 H. Dlugónska, *Ann. Parasitol.*, 2015, **61**, 299–301.

14 T. Efferth, S. Zacchino, M. I. Georgiev, L. Liu, H. Wagner and A. Panossian, *Phytomedicine*, 2015, **22**, A1–A3.

15 A. Alamgir, in *Therapeutic Use of Medicinal Plants and Their Extracts*, Springer, 2017, vol. 1, pp. 177–293.

16 T. A. Oliveira, M. B. Santiago, V. H. Santos, E. O. Silva, C. H. Martins and A. E. Crotti, *Chem. Biodiversity*, 2022, **19**, e202200097.

17 R. D. Bidgoli, *J. Food Sci. Technol.*, 2021, **58**, 1313–1318.

18 Y.-r. Zhao, G.-a. Zou and H. A. Aisa, *Phytochemistry*, 2022, **197**, 113108.

19 J.-H. Ahn, E.-J. Song, D.-H. Jung, Y.-J. Kim, I.-S. Seo, S.-C. Park, Y.-S. Jung, E.-S. Cho, S. H. Mo and J. J. Hong, *Phytomedicine*, 2022, **99**, 153934.

20 D. Bisht, D. Kumar, D. Kumar, K. Dua and D. K. Chellappan, *Arch. Pharmacal Res.*, 2021, **44**, 439–474.

21 T. A. Mohamed, H. A. Albadry, A. I. Elshamy, S. H. Younes, A. A. Shahat, M. T. El-wassimy, M. F. Moustafa and M. E. F. Hegazy, *J. Chin. Chem. Soc.*, 2021, **68**, 338–342.

22 T. A. Mohamed, A. A. Abd El Aty, A. A. Shahat, N. S. Abdel-Azim, K. A. Shams, A. A. Elshamy, M. M. Ahmed, S. H. Youns, T. M. El-Wassimy and S. A. El-Toumy, *Nat. Prod. Res.*, 2021, **35**, 1959–1967.

23 T. A. Mohamed, M.-E. F. Hegazy, A. A. Abd El Aty, H. A. Ghabbour, M. S. Alsaid, A. A. Shahat and P. W. Paré, *J. Asian Nat. Prod. Res.*, 2017, **19**, 1093–1101.

24 T. Usha, D. Shanmugarajan, A. K. Goyal, C. S. Kumar and S. K. Middha, *Curr. Top. Med. Chem.*, 2017, **17**, 3296–3307.

25 G. V. De Socio, P. Rubbioni, D. Botta, E. Cenci, A. Belati, R. Paggi, M. B. Pasticci and A. Mencacci, *J. Global Antimicrob. Resist.*, 2019, **19**, 154–160.

26 M. Frieri, K. Kumar and A. Boutin, *J. Infect. Public Health*, 2017, **10**, 369–378.

27 E. M. Mohi El-Deen, E. A. Abd El-Meguid, S. Hasabelnaby, E. A. Karam and E. S. Nossier, *Molecules*, 2019, **24**, 3650.

28 B. Li and T. J. Webster, *J. Orthop. Res.*, 2018, **36**, 22–32.

29 D. C. Kaur and S. S. Chate, *J. Glob. Infect. Dis.*, 2015, **7**, 78.

30 G. Teitzel, *Trends Microbiol.*, 2019, **27**, 285–286.

31 A. H. Al-Nadaf, S. A. Salah and M. O. Taha, *Comput. Biol. Chem.*, 2018, **74**, 263–272.

32 E. H. Reda, Z. T. A. Shakour, A. M. El-Halawany, E.-S. A. El-Kashoury, K. A. Shams, T. A. Mohamed, I. Saleh, A. I. Elshamy, M. A. Atia and A. A. El-Beih, *Antibiotics*, 2021, **10**, 252.

33 H. Mohsen and F. Ali, *Molecules*, 2009, **14**, 1585–1594.

34 A. E.-H. H. Mohamed, M. El-Sayed, M. E. Hegazy, S. E. Helaly, A. M. Esmail and N. S. Mohamed, *Rec. Nat. Prod.*, 2010, **4**.

35 M. Laid, M.-E. F. Hegazy, A. A. Ahmed, K. Ali, D. Belkacemi and S. Ohta, *Phytochem. Lett.*, 2008, **1**, 85–88.

36 S. M. Salah and A. K. Jäger, *J. Ethnopharmacol.*, 2005, **97**, 145–149.

37 M. M. Mokhtar, H. M. Shaban, M. E.-a. F. Hegazy and S. S. Ali, *Bull. Fac. Pharm. Cairo Univ.*, 2017, **55**, 195–201.

38 I. Kadi, M. Ouinten, N. Gourine and M. Yousfi, *Nat. Prod. Res.*, 2019, **33**, 875–878.

39 S. Amkiss, A. Dalouh and M. Idaomar, *Arab. J. Chem.*, 2021, **14**, 102976.

40 J. A. Marco, J. F. Sanz-Cervera, V. Garcia-Lliso, M. Guara and J. Vallès-Xirau, *Phytochemistry*, 1997, **45**, 751–754.

41 J. A. Marco, *Phytochemistry*, 1989, **28**, 3121–3126.

42 C. Narayanan and N. Venkatasubramanian, *J. Org. Chem.*, 1968, **33**, 3156–3162.

43 A. Ajmal, J. Wu and A. Tulak, CN114292253A, 2022.

44 E. D. McArthur, *Proc. RMRS*, 1998, **67**.

45 J. Valles and E. D. McArthur, *USDA Forest Service Proceedings RMRS-P-21*, 2001, pp. 67–74.

46 D. Podlech, *Compositae 'VI-'Anthemideae*, Akademische Druck-und Verlagsanstalt, 1986.

47 E. D. McArthur, C. L. Pope and D. C. Freeman, *Am. J. Bot.*, 1981, **68**, 589–605.

48 Y. R. Ling, *Bull. Bot. Res.*, 1991, **11**, 1–40.

49 Y. R. Ling, *Advances in Compositae Systematics*, 1995, pp. 283–291.

50 K. Bremer and A. A. Anderberg, *Asteraceae: cladistics and classification*, 1994.

51 L. E. Watson, P. L. Bates, T. M. Evans, M. M. Unwin and J. R. Estes, *BMC Evol. Biol.*, 2002, **2**, 1–12.

52 S. Zahra, M. Iraj, A. Mostafa and N. Taher, *J. Biodivers. Environ. Sci.*, 2014, **5**, 608–624.

53 R. Segal, L. Eden, A. Danin, M. Kaiser and H. Duddeck, *Phytochemistry*, 1985, **24**, 1381–1382.

54 R. Segal, I. Feuerstein and A. Danin, *Biochem. Systemat. Ecol.*, 1987, **15**, 411–416.

55 M. M. Gordon, D. Van Derveer and L. H. Zalkow, *J. Nat. Prod.*, 1981, **44**, 432–440.

56 A. Ahmed, M. Abou-El-Ela, J. Jakupovic, A. S. El-Din and N. Sabri, *Phytochemistry*, 1990, **29**, 3661–3663.

57 A.-u. Rahman, *Studies in natural products chemistry*, Elsevier, 2015.

58 J. Marco and O. Barbera, *Stud. Nat. Prod. Chem.*, 1990, **7**, 201–264.

59 T. Tutin, K. Persson and W. Gutermann, *Flora europaea*, 1976, 4, pp. 178–186.

60 J. F. Sanz, G. Castellano and J. A. Marco, *Phytochemistry*, 1990, **29**, 541–545.

61 J. Vallès and M. Torrell, *Fontqueria*, 1996, 44, pp. 17–24.

62 T. A. Farazi, J. K. Manchester, G. Waksman and J. I. Gordon, *Biochemistry*, 2001, **40**, 9177–9186.

63 R. Khalil, S. Ashraf, A. Khalid and Z. Ul-Haq, *ACS Omega*, 2019, **4**, 13658–13670.